The Iraqi Journal for Mechanical and Material Engineering, Vol.24, No1, May. 2025.

UTILIZING MICROWAVE TECHNOLOGY IN DESIGNING AN ELECTROMAGNETIC SENSING SYSTEM FOR ANALYZING MULTIPHASE FLOW DYNAMICS IN OIL AND GAS APPLICATIONS

Anwer A. Abass[1]
anwar.eali.engh472@student.uobabylon.edu.iq
[1]University of Babylon, Babylon

Dhirgham Alkhafaji[2]
eng.d.alkafagiy@uobabylon.edu.iq
[2]University of Babylon, Babylon

Stephen R. Wylie[3]
S.R.Wylie@ljmu.ac.uk
[3]Liverpool John Moores University

ABSTRACT

This research focuses on studying gas-liquid flow phenomena in engineering applications by de-signing and developing an advanced electromagnetic sensing system utilizing microwave technology. The objective is to analyze multi-phase flow characteristics and determine volume fractions within the oil and gas industry. A horizontal pipe model was used, featuring a non-intrusive cylindrical sensor, with LabVIEW software which has been employed for real-time data acquisition, processing, and visualization of results. Additionally, to analyze the electromagnetic behavior of the multiphase flow, Experimental measurements were conducted that the electromagnetic reflection coefficient S22 is strongly correlated with changes in the fuel (oil) ratio inside the pipe, particularly within the frequency range of 2.6 to 3.3 GHz. After validating the results through a simulation study using the HFSS program, it was further observed that increasing the air flow rate caused a significant change in the electromagnetic wave response. Consequently, fluid flow measurement was identified as an alternative to the traditional method. These results demonstrate the system's capability to effectively track flows in various scenarios. Moreover, the direct comparison between the obtained and calculated data showed a similarity of approximately 85%, demonstrating the adequacy of the applied theoretical model in characterizing the mixture flow behavior. This work presents a novel and effective method for determining the oil-to-air ratio, which can enhance electro-sensing approaches in real-world environments.

Keywords: Multiphase, microwave sensor, dynamic flow.

NOMENCLATURE

Symbol	Meaning	Unit
S22	Electromagnetic reflection coefficient, used to analyze the effects of fluid ratio variations in pipes.	Dimensionless

Received: January 18, 2025.
Accepted: April 06, 2025.

f_{mnp}	Resonant frequency for transverse magnetic (TM) or transverse electric (TE) modes.	(Hz)
X_{mn}	Zero value of the Bessel function, used in calculating the resonant frequency.	Dimensionless
X'_{mn}	First derivative of the Bessel function, used for calculating the resonant frequency for TE modes.	Dimensionless
μ_r	Relative permeability of the material, defining the material's response to magnetic fields.	Dimensionless
ε_r	Relative permittivity of the material, defining the material's response to electric fields.	Dimensionless
k_0	Wavenumber in free space, representing the relationship between wavelength and frequency.	(1/m)
E	Electric field at a specific point within the system.	(V/m)
H	Magnetic field induced by the electric field.	(A/m)
W_n	Test function used to represent the electric field in the finite element method (FEM).	Dimensionless
c	Speed of light in free space, used in calculating resonant frequencies.	(m/s)
R	Radius of the cylindrical cavity used in measurements.	(m)
L	Height of the cylindrical cavity used in measurements.	(m)
dB	Decibel, a unit used to measure the reflection coefficient (S22) and signal intensity.	(dB)
ω	Angular frequency, representing the relationship between frequency and time.	(rad/s)
$\nabla \times$	Curl operator, used to calculate variations in electromagnetic fields.	Dimensionless
$\int_V$	Volume integral, used to compute field properties within the studied region.	(m3)
$\int_S$	Surface integral, used to account for boundary effects in the system.	(m2)

INTRODUCTION

Techniques of measurement for multiphase flow are very important in the oil and gas industry, playing a vital role in production enhancement. Additionally, these techniques help minimize costs through real-time measurement of the flow rate of oil, gas, and water. (Deng, 2023), a significant number of studies indicate that multiphase flow meters deliver precise readings and provide higher-quality information that supports resource management decisions. For instance, in the oil and gas industry, flow rate estimations heavily rely on density and velocity measurements, which are frequently employed by numerous flow measurement approaches, as illustrated by Khezzar et al. (Khezzar, 2020). Furthermore, the role of Artificial Neural Networks in improving accuracy and reducing production losses has been highlighted by Bahrami et al (Bahrami, 2024). has also investigated the measurement methods which influenced by factors such as density and conductivity, that can lead to weaker measurements in multiphase systems, as explained by Alimonti. (Alimonti, 2009). Locating flow patterns and measuring gas fractions have also been shown to be efficient using ultrasonic techniques, as stated by Carvalho et al. (Carvalho, 2016). The intention of this research paper is to provide an introduction to multiphase flow measurement approaches, their usage, and challenges, enabling an advanced understanding of this complex phenomenon.

Two-phase flow is commonly employed in chemical and mechanical engineering applications and in oil wells, power generation, reactors, boilers, condensers, evaporators, and combustion systems (Khorasani, 2017). Within the framework of comprehensive phenomenon analysis, an integrated theoretical framework for understanding the physical variables affecting flow dynamics is developed, including quantitative relationships between velocity ratios, fluid rheological properties, and interacting physical forces. (Liu, 2022) and Regan (2023) enhanced this understanding through their in-depth analytical studies of the physical mechanisms responsible for flow pattern transitions, emphasizing the pivotal role of surface shear forces in pattern formation. Combined, these findings represent a new breakthrough in industrial application performance attainment, opening new doors for optimizing operational efficiency and developing advanced methods related to the field of multiphase fluid engineering (Regan, 2023). Research on a cylindrical resonant cavity that operates in the frequency band of 1–6 GHz indicated that, in addition to a frequency shift, this cavity can sense the mixture ratio due to changes in resonant frequency as well as energy absorption (Oon, 2017). The electrical properties of the studies showed significant changes with an alteration in the oil-to-air ratio, which affects its capability to absorb EM energy. This subsequently leads to the resonant frequency in the cavity varying, which allows for the measurement of the exact component ratio in the mixture (Clegg, 1985).

Microwave sensors provide an innovative method for studying multiphase flows because they accurately measure properties of industrial flow systems without interrupting the process stream. Assessment technologies play an essential role in both flow behavior comprehension development and innovative oil and gas solutions research. For instance, the technology can be applied in industrial practices for non-contact sensing and measurement of mixture properties (Fantom, 1990). The results also indicated that the electromagnetic field in the range of 3-4 GHz is highly sensitive to changes in mixture ratios, making this technique technically suitable for applications requiring accurate and rapid measurements (AlFaouri, 2014). Dynamic multiphase flow dynamics is a critical research area in petroleum engineering and advanced industrial sectors. Recent experimental studies have demonstrated the non-linear dependence of airflow rates on flow patterns in two-phase flow systems. Wang et al. (2023) reviewed the physical phenomena of air velocity variations in an experimental system with a limited oil flow rate of 0.5 liters/minute. These results highlighted the stage-wise flow development, transitioning from stable stratified flow to waviness and finally to intermittent flow, with velocity changes (Wang, 2023)

The microwave sensors are essential for multiphase oil and air measurements that yield a new wave of technology involving real-time data acquisition with high accuracy. Frequency-modulated continuous wave radars (FMCW) have shown substantial benefits in oil droplet and air bubble velocity measurements, making them suitable for use in fast-changing environments. As a continuous wave radar (Sabzevari, 2020 and AlHosani, 2020), microwave resonators and time-domain reflectometry (TDR) sensors (sensors of insulation properties and concentrations of oil, air, etc.) improve sensitivity with invaluable measurements (Xie, 2009 and Al-Shamma'a, 2006). Furthermore, microwave interference measurements provide an additional degree of monitoring as phase shifts in the presence of multiphase flows are scrutinized to determine velocity and concentration with great fidelity (Al-Kizwini, 2013 and Alkhafaji D., 2018). The above technologies represent effective and non-intrusive methods of measuring flow in multiphase environments in the oil and gas sector (Ashton, 1994). Microwave sensor technology is considered one of the most advanced methods for monitoring two-phase flow, particularly in multi-phase flow systems where gas and liquid coexist in an annular configuration surrounding the liquid. Reviewing the work of Alkhafaji et al., sensors demonstrate a significant capability for measuring variations in electrical and mechanical properties. These measurements provide a chemical composition-independent assessment of the true phase proportions in mixtures. This new technology enhances insight into process dynamics under varying operating conditions, addressing the challenge of improving industrial process efficiencies and reducing costs (Alkhafaji D., 2018). The present work focuses on investigating the flow characteristics of oil in single-phase, multi-phase, and oil/gas mixtures across stages. It utilizes a horizontal pipe connected to a non-invasive setup.

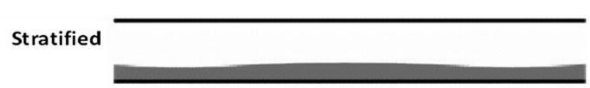

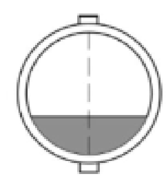

(a) (b)

Fig. 1.a. Regimes in Horizontal Multiphase Pipelines b. Stratified flow (30 % oil)

MODELING A CYLINDRICAL CAVITY SENSOR

The resonant frequency of cylindrical cavities is determined by applying boundary conditions to the electromagnetic field expressions, with the distinction that the frequencies of TE and TM modes differ. This analysis takes into account the cylinder's height, radius, and the electric boundary conditions at the enclosing plates, making it relevant for future applications involving electromagnetic waves (Pozar, 2005). The mathematical expressions for the resonant frequencies of transverse magnetic (TM) and transverse electric (TE) modes in a cylindrical waveguide are provided as follows (Collin, 2001 and Scott, 2005).

The resonant frequency for transverse magnetic (TM) modes is defined by Eq. (1).

$$f_{mnp} = \frac{c}{2\pi\sqrt{\mu_r \varepsilon_r}} \sqrt{\left(\frac{X_{mn}}{R}\right)^2 + \left(\frac{p\pi}{L}\right)^2} \qquad (1)$$

For transverse electric (TE) modes, the resonant frequency is given by Eq. (3.2).

$$f_{mnp} = \frac{c}{2\pi\sqrt{\mu_r \varepsilon_r}} \sqrt{\left(\frac{X'_{mn}}{R}\right)^2 + \left(\frac{p\pi}{L}\right)^2} \qquad (2)$$

Equation (1) is utilized in this study, as the TE mode is generated within the cavity. Here, , (X_{mn}) denotes the zero value of the Bessel function, while (X'_{mn}) represents its first derivative. The experimental setup features a Horizontal brass cylinder cavity (sensor) designed at the Ministry of Science for equation (2) employed in this paper to generate TE mode in a brass cylinder cavity which is designed by the experts (Ministry of Science and Technology's Department of Industrial Research and Development. The cavity has a diameter of 30 mm and depth of 120 mm, including two cutaways (P_1), and (P_2) (at 15 mm diameter) for antenna coupling(P_1) ,transmission and(P_2) , reception. Finally dual 1.5 cm diameter upper ridge for easy sample tube entry to lose minimum electrical field. However, dielectric loss is directly proportional to penetration depth as well; brass a known metal with extremely good reflectivity in microwave region is so light and cheap for practical applications as shown figure 2. The chart shows the dielectric loss factor versus the energy absorption rate per unit volume in order to develop an understanding regarding the design of cylindrical cavities for microwave uses. High purity materials, for example, thermoplastics, and liquid resins are transparent to microwaves while materials with a moderate dielectric loss, water, are highly absorbing of microwaves where strong signal has to be coupled to microwaves. While, the materials with high dielectric loss like steel they do reflect energy and used in insulation. Therefore, from this study it is possible to design cylindrical cavities made of brass to improve performance by using the right material and suitable geometrical dimensions to maximize coupling to electromagnetic waves and further research to determine the effect of further geometrical parameters as figure 3 (Sheen, 2007)

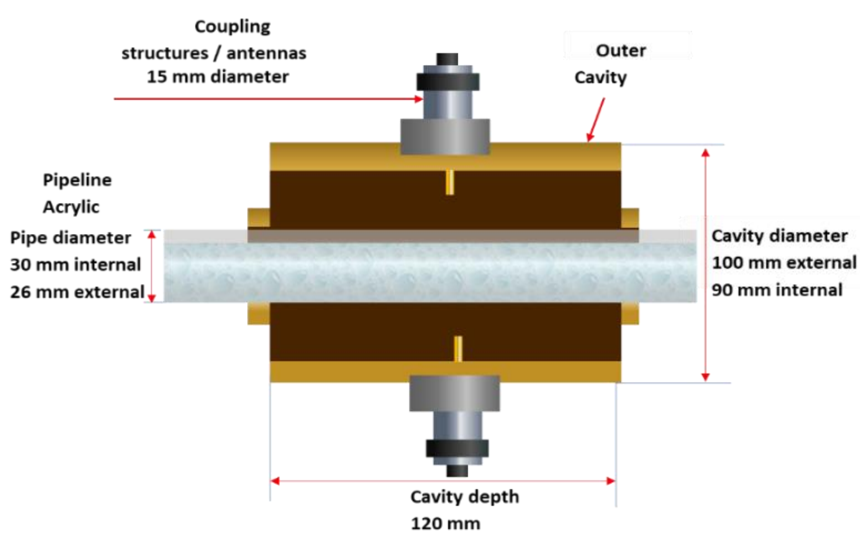

Fig. 2. Schematic representation of the cavity sensor along with the coupling structures.

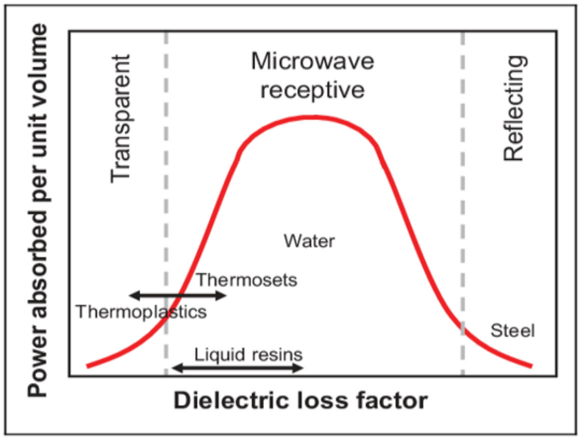

Fig.3.The relationship between the power absorbed per unit volume and the dielectric loss factor of different materials (Thostenson, 1999).

EXPERIMENTAL STUDY

After preparing the sample and selecting the dimensions based on previous studies, the experimental setup was designed using a cylindrical cavity tailored to the diameters of the tubes under investigation. Diameters of 2 cm and 4 cm were selected for horizontal flow testing, with experiments conducted at the Ministry of Science and Technology, Department of Industrial Research and Development Laboratory. The sample preparation included constructing a horizontal cylindrical cavity made of brass, with variable diameters corresponding to the tube under study. Additionally, a pump was incorporated into the system to facilitate the flow of the oil-air mixture through the tube, as depicted in Figures 4 and 5. The cavity sensor device was connected to an Agilent network analyzer operating within the frequency range of 2–4 GHz. The network analyzer was linked to Port 1 (P1) and Port 2 (P2) using precision cables and appropriate adapters. Table (2) provides a detailed list of the primary components used in the system for analyzing the flow and properties of the oil-air mixture, utilizing advanced measurement tools. The equations are written in Math Type, or equation editor size 12pt, with consecutive numbering.

Fig.4. Experimental setup.

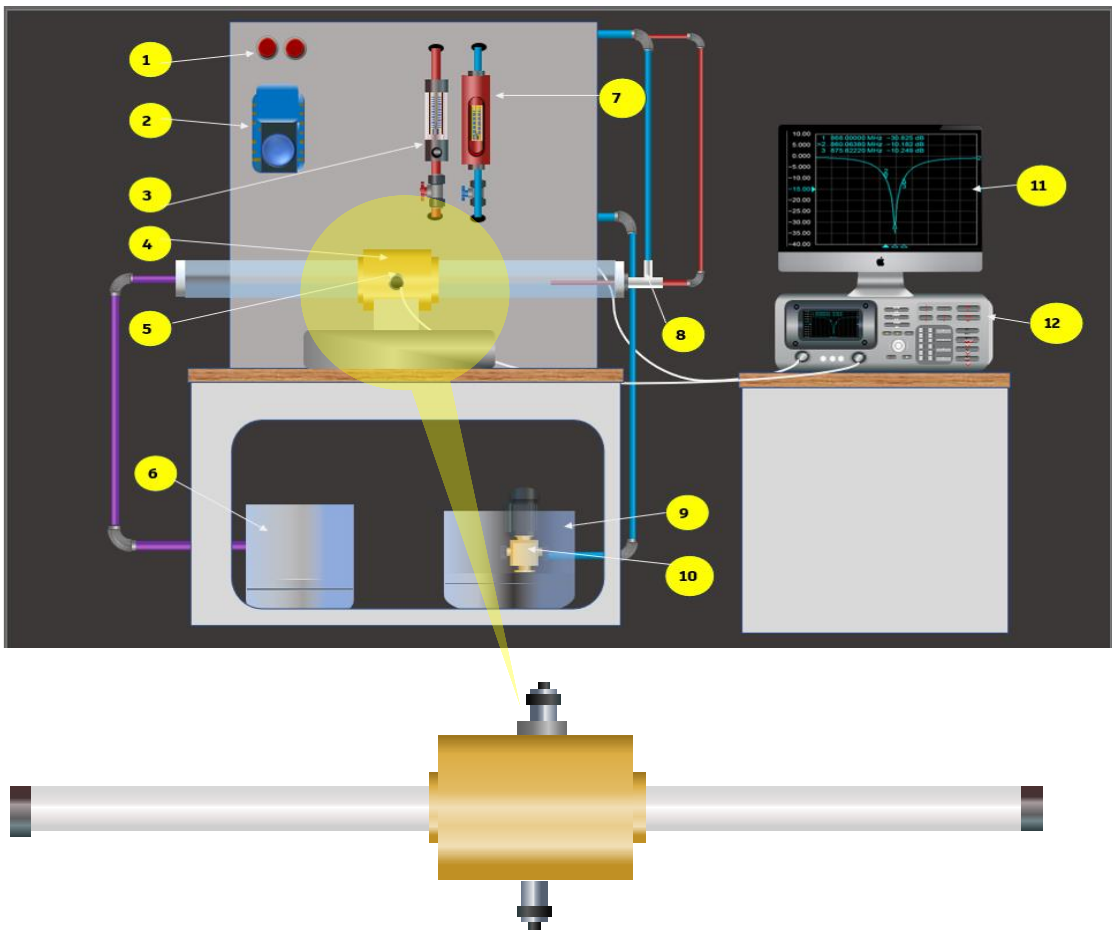

Fig.5. Schematic diagram of the experimental

Table 1. Component the part of the rig.

No.	Component
1	control Switch
2	air supply by compressor

3	Water flowmeter
4	Cavity cylindrical sensor
5	Waveguide adapter with a dipole antenna
6	Received Tank.
7	Flowmeter
8	Divide the mixture
9	mixture Tank (PEG & Water)
10	Pump
11	Computer
12	Vector Analyzer

The cylindrical resonant body was chosen and manufactured solely in practical testing due to the difficulties encountered in producing vacuum resonant bodies with spherical shapes and others in Iraq. Copper was the chosen material for this vacuum resonant body's construction, comprising approximately 67% copper and 33% zinc. There are numerous advantages derived from using copper, such as its high Q value, and some resonant bodies have low losses and high accuracy in measurements. Nevertheless, flaws particularly associated with the cost of such materials increase as the size grows and the production period lengthens. When the size of a vacuum resonant body is large and heavy, a metal or alloy with little density is used to cut costs. To minimize the density impact (external surface), some designers use silver to coat the inside surface of the used vacuum. Figure 6 below illustrates the proposed practical cylindrical vacuum body, which was designed and used in the tests of this letter. The cylindrical resonator was designed from a copper alloy, and a lathe was used to machine the cavity. Likewise, the cover's hole comes in different diameters, which align with the diameter of the tubing used for the flow, For the part, the cylinder is drilled from the top with a 4 cm hole to pass an acrylic rod, and from the side, it is drilled with a diameter of 10 cm on two opposite sides for mounting a Waveguide adapter with a dipole antenna as figure 7.

Fig.6. Fabricated cylindrical cavity resonator.

Fig. 7. Hole in fabricated cylindrical cavity resonator for side view and top view.

SIMULATION STUDY

A simulation study was conducted using the ANSYS Workbench 2022 R1 software, which is known for its ability to compute the electromagnetic behavior of multiphase flow mixtures. The subsequent analysis of the program code provides a detailed analysis of the behavior of the two-phase (oil and gas) flow mixture. ANSYS Twin Builder 2022 R1 (HFSS) is used to calculate the natural modes, or free vibrations, of a given structure. ANSYS Workbench is based on the finite element method to calculate the free vibrations of the model based on the geometry, materials, and boundaries. The ANSYS Twin Builder 2022 R1 (HFSS) simulation code is typically used to capture the electromagnetic field inside the structure. Although its implementation is largely transparent, a general understanding of the method is beneficial for the more effective use of ANSYS Twin Builder 2022 R1 (HFSS).

It was Obvious that the ANSYS Twin Builder 2022 R1 (HFSS) program has been designed to compute the electromagnetic behavior of multiphase mixture components, and therefore the program needs to be rebuilt for our purposes in finding the transition in harmonic frequencies due to the change in component ratios (oil and gas) and the flow system. For applied flow systems, the design of the cavity simulation can be achieved by imagining the flow shape within the pipe, so Two parallel layer have been proposed to within the cavity pipe to represent the two phases in the applied flow system, assuming no mixing between the phases. The change in fraction ratios can be achieved by changing the areas of the two parallel layers (sections), and then assigning material properties to these two sections to achieve the representative permeability of the required phases (oil and gas). The design is then complete, and the simulation can be started.

GOVERNING EQUATIONS

Reflection Coefficient (S22): A Complete Study of Electric and Magnetic Fields Governing Equations in HFSS with Errors (Cendes I., 2008 and Cendes D., 2001)

1. Electric field equation:

$$\nabla \times \left(\frac{1}{\mu_r} \nabla \times E\right) - k_0^2 \varepsilon_{rE} = 0 \qquad (3)$$

Here, the basics of this equation provide a way to account for the electric field E at a point and the properties of the surrounding medium with particular materials.

2. Magnetic field equation:

$$H = \frac{1}{\omega\mu} \nabla \times E \qquad (4)$$

This equation relates the magnetic field H with the electric field E,and it is used to calculate H upon arrival.

3. Integral equation for the solution:

$$\int_V W_n \cdot \nabla \times \left(\frac{1}{\mu_r} \nabla \times E\right) - k_0^2 \varepsilon_r W_n \cdot (E) dV = 0 \qquad (5)$$

This integral equation forms the foundation of the finite element method (FEM) implemented in HFSS to solve governing equations.

4. Integral equation actual meaning - after mathematical model introduction:

$$\int_V \left(W_n \cdot \nabla \times \left(\frac{1}{\mu_r} \nabla \times E\right) - k_0^2 \varepsilon_r W_n \cdot E\right) dV = \int_S (\text{boundary terms}) dS \qquad (6)$$

This equivalent formula is used for the numerical treatment of surface boundaries, as it transforms the integral equation.

5. E field representation with the help of test functions:

$$\boldsymbol{E} = \sum x_m W_m \qquad (7)$$

The electric field E is represented in terms of test functions W_n and column vectors x_m, which are determined by this equation.

6. Matrix form of integral equation:

$$\sum x_{m} \int_V \left[(\nabla\times W_n)\cdot\left(\frac{1}{\mu_r}\nabla\times W_m\right)-k_0^2 W_n\cdot W_m\right]dV = \int_S (\text{boundary terms})dS \qquad (8)$$

This expression provides the matrix formula to calculate the $x_m$coefficients according to FEM.

7. Reflection coefficient S_{22} expression:

$$S_{22} = \frac{\sum x_{\int_S} \mathrm{b}W_m\cdot dl}{\sum x_{\prime} \int_S \mathrm{b}W_{m^{\prime}}\cdot dl} \qquad (9)$$

This equation provides the dipole moment and reflection coefficient S_{22}.

A denotes the border condition. The matrix is N×N and represents the relationship between current and voltage sources, port excitation, and the incidence wave vector. Once the value of x has been known, E can be calculated using equations (7). The HFSS solution steps follow a straightforward, direct, and iterative procedure. This suggests perform the previously mentioned procedure step iteratively, thoroughly investigating various mesh configurations until obtain the correct field solution. refer to the iterative process of finding a solution in HFSS as an adaptive technique. Typically, an adaptive process will yield precise outcomes at a superior level. The following section will provide a comprehensive analysis of the steps above. After doing HFSS calculations, can determine the port excitation cross-section modes present in a waveguide within a simple design framework. (Ansys Ansoft HFSS-User Guide, 2009 and Ansoft, 2009) for main Steps for Simulation Using HFSS As illustrated in figure 8.

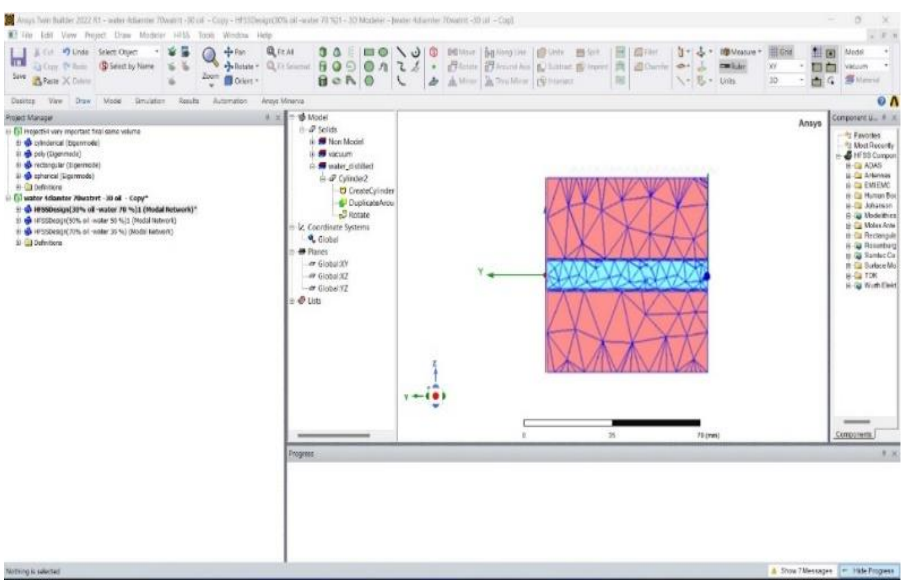

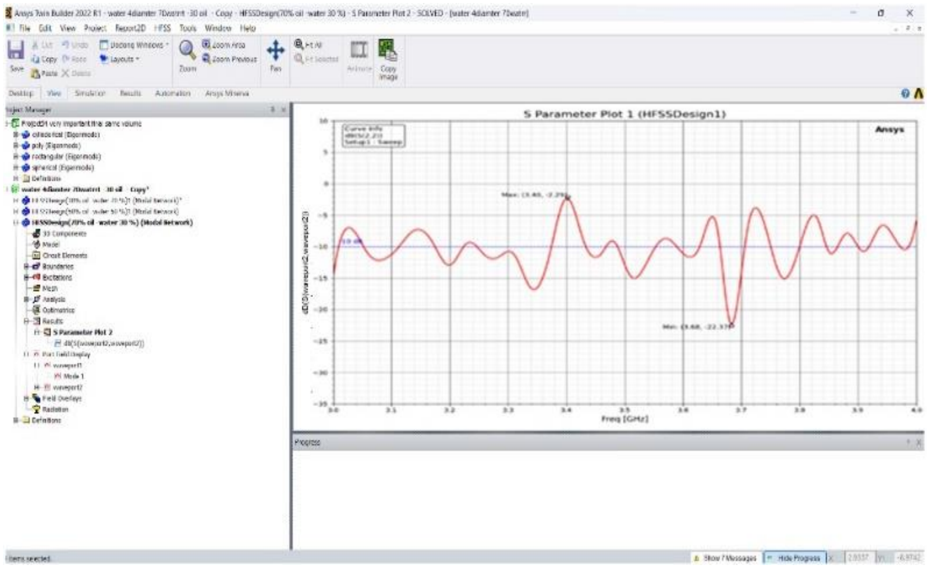

Figure 8: Main Step for Simulation using HFSS.

THE VALIDATION OF THE HFSS SIMULATION RESULTS

The validation of the HFSS simulation results was performed by comparing the simulated and experimental resonant response with respect to the oil hold-up level of the two-phase (oil/air) mixture, which represents a simple stratified flow regime within the pipe. The experimental results were in good agreement with the theoretical predictions by HFSS, with some error due to the uncertainty of volume fraction and signal noise, for figure 9 shows that the comparison between the experimental and theoretical results for the oil-air (70 %) oil demonstrates a good agreement across the frequency range from 2.6 to 3.3 GHz. The trends in the variations of the reflection coefficient with frequency have been well-captured by the theoretical model, with only minor differences observed in the specific values. This close alignment between the results indicates that the theoretical model used in describing the flow dynamics of the mixture under the studied conditions is valid and can provide reliable estimates of the mixture's behaviour. The findings reinforce the credibility of the theoretical approach and its potential for enhancing processing and transportation techniques in the oil and gas industry.

Figure 9 illustrates the reflection coefficient (S_{22}) as a function of frequency for a tube with an internal diameter of 3 cm, filled with a 70% oil mixture. The variation of S_{22} in decibels (dB) across the frequency range of 2.6 GHz to 3.3 GHz is presented, where electromagnetic waves are shown to interact with the oil-air interface inside the tube. The reflection coefficient is observed to range from -15 dB to 8.903 dB, with significant reflection occurring at higher frequencies. This behavior is attributed to the dielectric properties of the mixture, where the relative permittivity of oil (ε_{oil} = 2.2–2.5) is considerably higher than that of air (ε_{air} =1). Sensitivity of the system to the mixture properties is particularly evident near 3.0 GHz, where the reflection coefficient reaches its minimum, primarily due to the gas composition. This highlights the influence of relative permittivity variations on the electromagnetic wave propagation characteristics. agreement between experimental data and theoretical predictions 85%shows an easy but not perfect match between in-situ data and modeling. Such results may be useful in studies of electromagnetic sensing improvements or material property characterization for industrial applications.

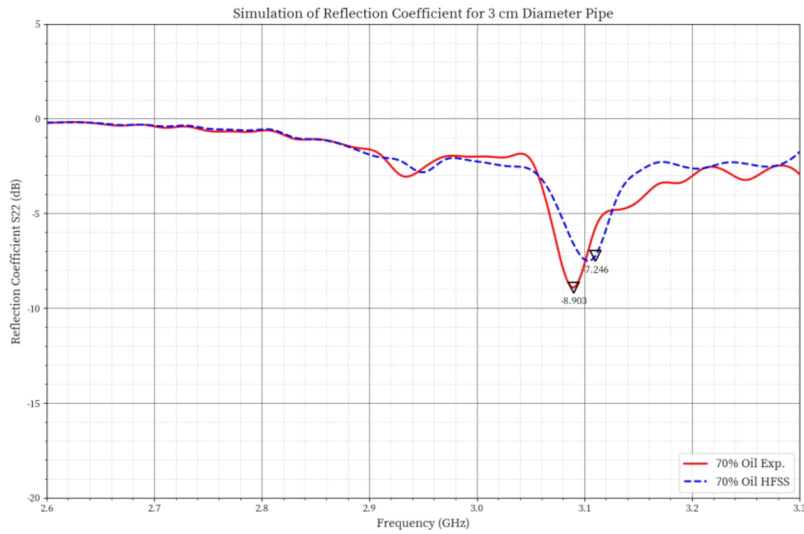

Fig. 9. Comparative Analysis of Experimental and Theoretical Performance of the Mix.4 (3 cm) Model at a Flow Rate of 1.5 L/min.

EXPERIMENTAL AND DISCUSSION

TWO-PHASE FLOW EXPERIMENT.

The experimental results demonstrate that the electromagnetic reflection coefficient (S_{22}) across the studied frequency range is highly sensitive to the fuel (oil) ratio within the pipe. The reflection coefficient, as a function of the fuel (oil) ratio inside the pipe, significantly influences the electromagnetic reflection coefficient, S22, within the investigated frequency range.

As shown in figure 8, at a 100 % fuel ratio, the minimum reflection coefficient value was observed at the 3.07 GHz frequency, measuring -9.49 dB and for a 70% fuel ratio, the minimum reflection coefficient value was observed at the 3.09 GHz frequency, measuring -8.9 dB. This represents a notable improvement in the matching between the electromagnetic signal and the propagating medium at this specific frequency, attributed to changes in the electrical permittivity and magnetic permeability of the medium induced by the increased fuel ratio.

At a 50% fuel ratio, a similar behavior was noted at a slightly lower frequency -8.07. However, for a 30% fuel ratio, the dispersion plot of the reflection coefficient exhibited a more stable overall shape with fewer fluctuations across the entire frequency range. This indicates that the impact of a low fuel ratio on the electrical properties of the medium is less pronounced compared to higher fuel ratios. The cylindrical cavity used in this study proved effective in accurately measuring the oil-to-air ratio. Variations in permittivity and permeability due to the fuel ratio are clearly reflected in the measured reflection coefficient, making this an accurate method for monitoring the fuel ratio in radiative systems.

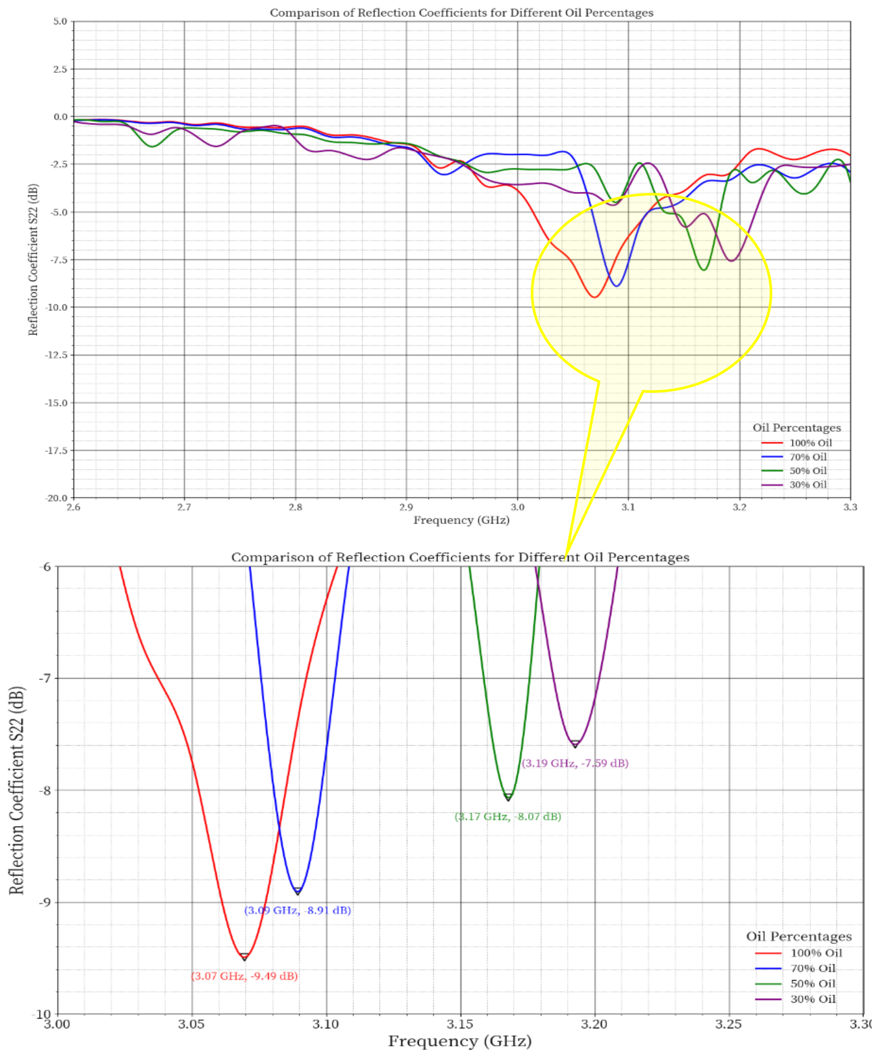

Fig.10. Analysis of Reflection Coefficient for flow (30, 50, 70) % oil through pipe diameter (3 cm) at 2.6 to 3.3 GHz.

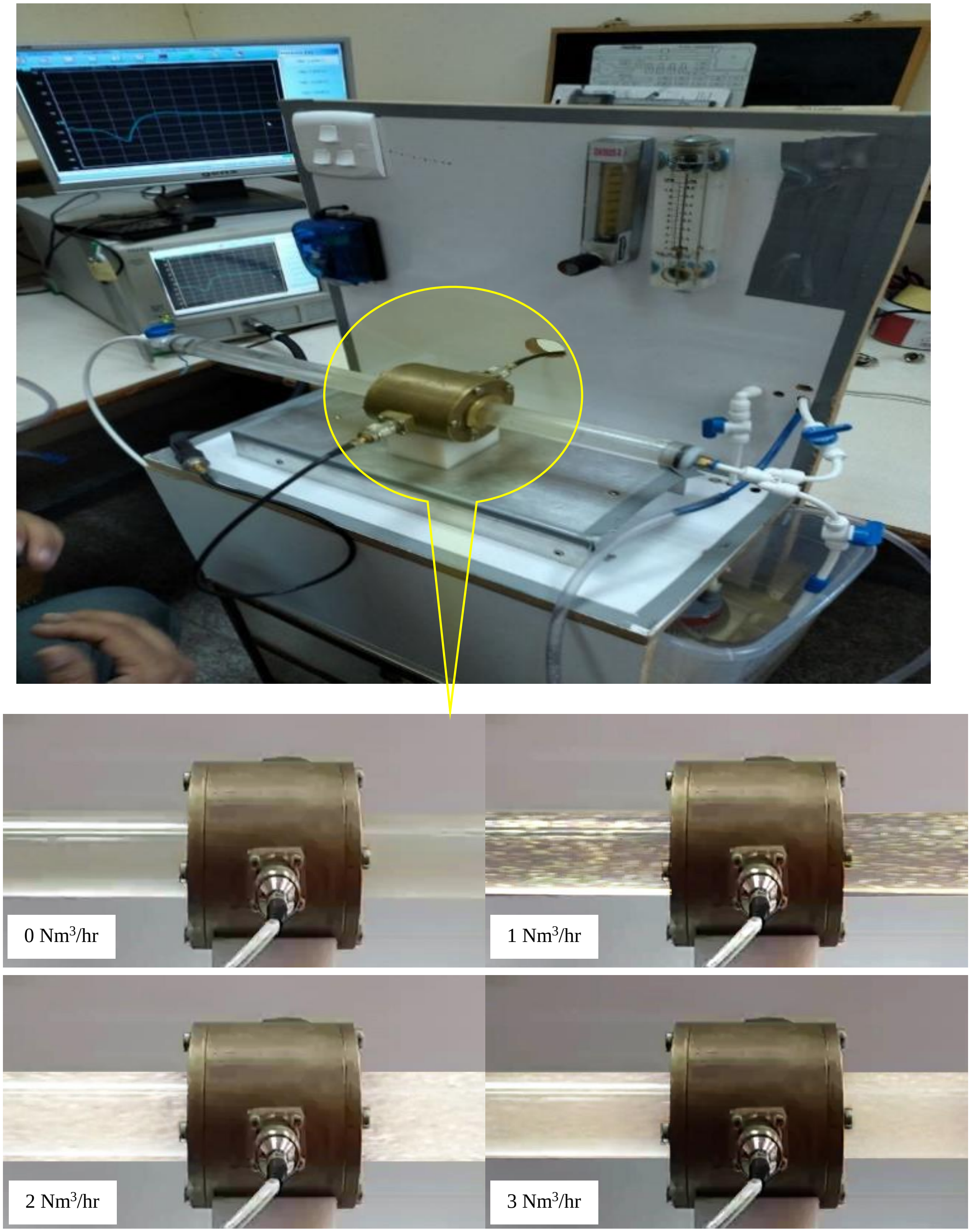

Fig.11. The homogenous flow created with various air input conditions.

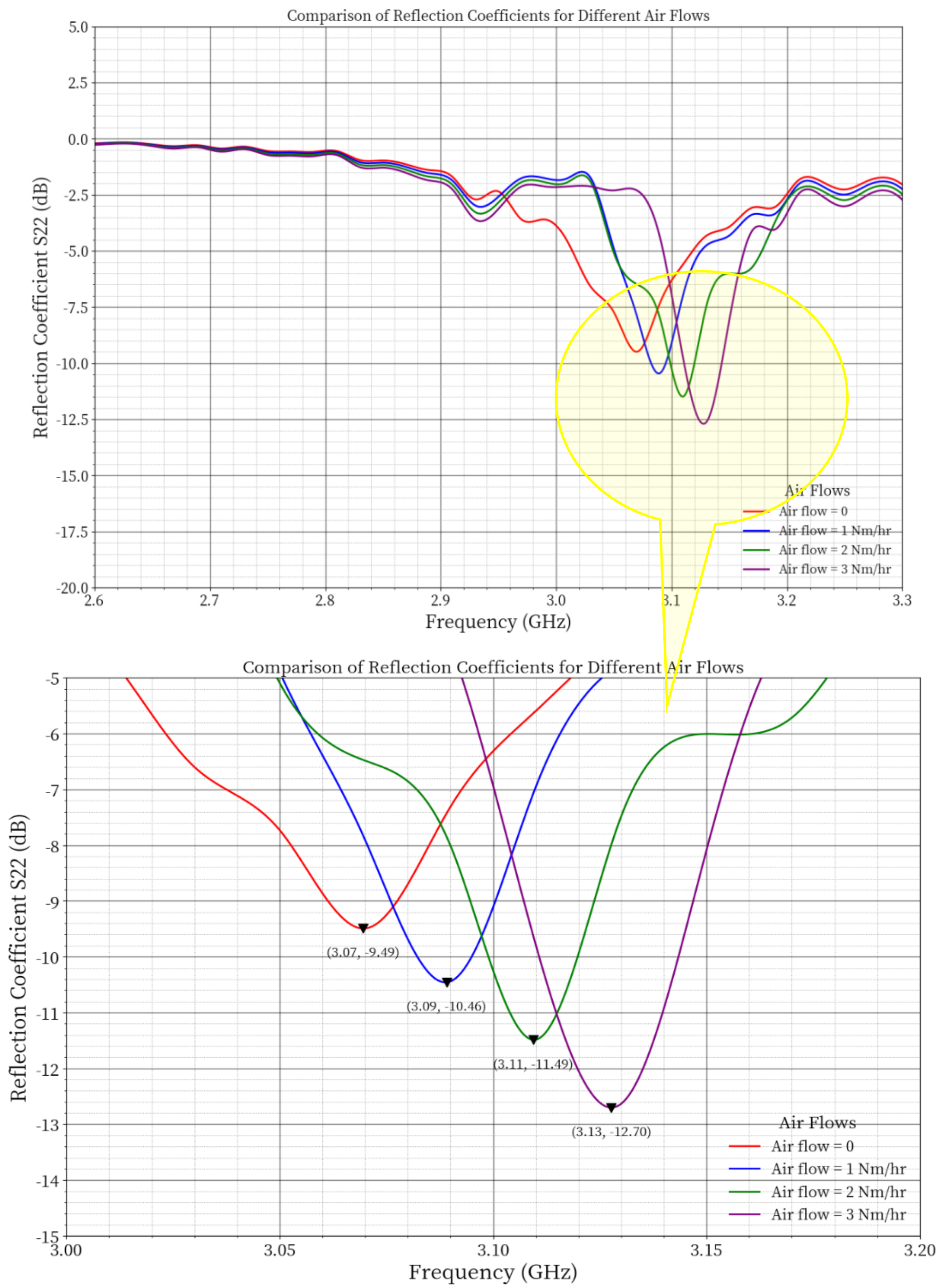

Fig.12. Graph illustrating the identification of homogeneous flow type with varying air input through the microwave response parameter S22.

Determination of reflection coefficients (S22) in various air flow changes in the microwave range due to the movement of plasma loom machinery as shown figure 12. The aim of this research is to characterize the consequences of specifying air flow variation within a specific system. S22 reflection coefficients have been measured in the 3 GHz to 3.2 GHz range at four settings: zero m/hr, 1 Nm/hr, 2 Nm/hr, and 3 Nm/hr. When results were recorded, noticeable spikes in the S22 values occurred at specific frequencies for all flow measurements. At zero flow, observed from a peak at -9.49 dB, 3.1050 GHz. The peak shifted to a higher frequency, and the S22 value decreased to -10.46 dB, -11.49 dB at 3.09 GHz, and -12.7 dB at 3.13 with increased air flow. These conclusions indicate that the characteristics of reflection are highly sensitive to variations in air flow within the system under investigation. This sensitivity can be utilized to optimize and improve systems that depend on air flow, such as cooling or ventilation systems. This data also serves as an empirical starting point for investigating the underlying effects of operational parameters on electromagnetic properties in other material systems.

The variations in the reflection coefficient with the fuel ratio reflect the impact of changes in the medium's electrical permittivity and magnetic permeability. As the fuel ratio increases, the matching between the electromagnetic signal and the medium improves due to significant alterations in the material properties, resulting in a lower reflection coefficient at specific frequencies. These findings enhance our understanding of the relationship between the physical properties of the medium and its electromagnetic behavior, paving the way for various industrial applications.

CONCLUSIONS

The study revealed that variations in the oil percentage within the pipe can be detected through a highly sensitive electromagnetic reflection coefficient (S_{22}). Monitoring this coefficient is crucial in industrial applications, and efforts should focus on enhancing RF measurements for improved accuracy. Experimental results showed excellent agreement with theoretical predictions, validating the model as an accurate representation of mixture flow behavior. This demonstrates the model's potential to enhance both processing and transportation methods in oil and gas platforms. Additionally, an increase in air input was observed to significantly affect the unsteady homogeneous sheath–streaming flow, influencing electromagnetic wave behavior. This opens up new opportunities for developing advanced measurement techniques to address fluid flow challenges in engineering. The technology created for evaluating the oil-to-air ratio offers a valuable tool for advancing electromagnetic sensing methods, improving material properties, and optimizing transportation processes across various industries.

RECOMMENDATIONS

Enhance models and sensor sensitivity, integrate AI for data analysis, expand industrial applications, develop portable systems, and test on complex multiphase flows to improve performance.

FURTHER WORK

The methodologies can be generalized for future work by refining models, improving sensing technologies, and adapting them to more complex systems and diverse industrial environments.

REFERENCE

Al-Kizwini, M. and Al-Kizwini, S., 'The Monitoring of the Two-Phase Flow-Annular Flow Type Regime Using Microwave Sensor Technique', Measurement, Vol.46, No.1, pp. 45-51, 2013.

AlFaouri, Y. S., Microwave technique for monitoring fluid level in the horizontal petroleum carrying pipeline (M.Sc. Thesis), King Fahd University of Petroleum and Minerals, Saudi Arabia, 2014.

Alkhafaji, D., 'Application of Microwave Analysis to Monitoring Slug Flow in Pipeline Networks', Instrumentation Mesure Métrologie, Vol.17, pp. 479-489, 2018.

Alkhafaji, D., 'Experimental and Numerical Study for Multi-Phases Flow Measurement by Microwave Cavity', International Journal for Research in Applied Science and Engineering Technology, Vol.6, pp. 2924-2929, 2018.

AlHosani, M. M., 'Multiphase Flow Meters Targeting Oil & Gas Industries', Measurement, Vol.165, 108111, 2020.

Al-Shamma'a, S. R., 'RF Sensor for Multiphase Flow Measurement Through an Oil Pipeline', Measurement Science and Technology, Vol.17, pp. 2141, 2006.

Ansoft, An Introduction to HFSS™, Fundamental Principles, Concepts, and Use, Ansoft, LLC, 2009.

Ansys, Ansys Ansoft HFSS-User Guide, Ansys, 2009. [Online]. Available: https://www.ansys.com/products/electronics/ansys-hfss

Ashton, S. L., 'Development and Trial of Microwave Techniques for Measurement of Multiphase Flow of Oil, Water and Gas', SPE Asia Pacific Oil and Gas Conference, SPE-28814-MS, 1994.

Bahrami, S., 'Application of Artificial Neural Network to Multiphase Flow Metering: A Review', Flow Measurement and Instrumentation, Vol.0955-5986, 2024.

Carvalho, M. F., 'The Use of an Ultrasonic Technique and Neural Networks for Identification of the Flow Pattern and Measurement of the Gas Volume Fraction in Multiphase Flows', Experimental Thermal and Fluid Science, Vol.70, pp. 29-50, 2016.

Cendes, D. F. and Smith, I. B., 'Total and Scattered Field Formulations in the Transfinite Element Method', Vol.44, pp. 778-781, 2008.

Cendes, D. F. and Smith, K. S., 'ALPS: A New Fast Frequency-Sweep Procedure for Microwave Devices', IEEE Transactions on Microwave Theory and Techniques, Vol.49, pp. 398-402, 2001.

Clegg, I. M., Microwave Techniques for the Detection of Water in Crude Oil (Ph.D. Thesis), The University of Manchester, United Kingdom, 1985.

Collin, R., Fundamentals for Microwave Engineering, 2nd edition, IEEE Press, 2001.

Deng, F., 'Online Measurement and Analysis Technology of Oil & Gas Multiphase Flow by Magnetic Resonance', International Petroleum Technology Conference, p. D022S025R003, 2023.

Fantom, A., Radio Frequency & Microwave Power Measurement, IET, 1990.

Giuseppe, F. A., 'Multiphase Flow Metering', Developments in Petroleum Science, Vol.54, pp. 47-190, 2009.

Khorasani, S. A., 'Effect of Air Bubble Injection on the Performance of a Horizontal Helical Shell and Coiled Tube Heat Exchanger: An Experimental Study', Applied Thermal Engineering, Vol.111, pp. 676-683, 2017.

Khezzar, M. M., 'An Ultrasonic-Based Multiphase Flow Composition Meter', Measurement, Vol.161, 107806, 2020.

Liu, J., 'A Simulation Investigation of Lubricating Characteristics for a Cylindrical Roller Bearing of a High-Power Gearbox', Tribology International, Vol.167, 107373, 2022.

Oon, C. S., Non-Invasive Electromagnetic Wave Sensor for Flow Measurement and Bi-phase Application (Ph.D. Thesis), Liverpool John Moores University, United Kingdom, 2017.

Pozar, D. M., Microwave Engineering, John Whiley & Sons, Inc., 2005.

Regan, N. J., The Characterisation of Liquid Sprays Injected from Circular and Non-Circular Nozzles into High-Speed Subsonic Cross-Airstreams (Ph.D. Thesis), University of Sussex, 2023.

Sabzevari, F. M., 'A Microwave Sensing and Imaging Method for Multiphase Flow Metering of Crude Oil Pipes', IEEE Journal of Selected Topics in Applied Earth Observations and Remote Sensing, Vol.13, pp. 1286-1297, 2020.

Scott, A. W., Understanding Microwaves, John Wiley & Sons Inc., 2005.

Sheen, J., 'Microwave Measurements of Dielectric Properties Using a Closed Cylindrical Cavity Dielectric Resonator', IEEE Transactions on Dielectrics and Electrical Insulation, Vol.14, No.5, pp. 1139-1144, 2007.

Thostenson, E., 'Microwave Processing: Fundamentals and Applications', Composites Part A: Applied Science and Manufacturing, Vol.8, pp. 1055-1071, 1999.

Wang, J., 'Experimental Investigation on Separation Characteristics of Axial Cyclone Separator', Science China Technological Sciences, Vol.66, pp. 3231-3244, 2023.

Xie, Z., 'Microwave-Tomographic System for Oil- and Gas-Multiphase-Flow Imaging', Measurement Science and Technology, Vol.20, 104026, 2009.